THE JOURNAL OF PHYSICAL CHEMISTRY B

ARTICLE

pubs.acs.org/JPCB

Effect of Protein Environment on Electronically Excited and Ionized States of the Green Fluorescent Protein Chromophore

Ksenia B. Bravaya,[†] Maria G. Khrenova,[‡] Bella L. Grigorenko,[‡] Alexander V. Nemukhin,[‡,§] and Anna I. Krylov*[,†]

[†]Department of Chemistry, University of Southern California, Los Angeles, California 90089-0482, United States

[‡]Department of Chemistry, M.V. Lomonosov Moscow State University, Moscow 119991, Russia

[§]N.M. Emanuel Institute of Biochemical Physics, Russian Academy of Sciences, Moscow 119334, Russia

Supporting Information

ABSTRACT: The effect of the protein environment on the electronic structure of the green fluorescent protein (GFP) chromophore is investigated by QM/MM (quantum mechanics/molecular mechanics) calculations. The protein has very small effect on the excitation energy of the bright absorbing and the lowest triplet states of the anionic GFP chromophore, deprotonated 4-hydroxybenzylidene-2,3-dimethylimidazolinone (HBDI) anion, however, it increases vertical detachment energy from 2.5 eV (gas-phase deprotonated HBDI anion) to 5.0 eV (solvated protein). We also investigated possible existence of the charge-transfer-to-solvent (CTTS) states associated with the GFP chromophore. Although precursors of such states appear in cluster calculations, a tightly packed structure of the protein prevents the formation of the CTTS states in this system. Motivated by a recently discovered new type of photoconversion, oxidative redding, we characterized the redox properties of GFP. The computed standard reduction potential of the anionic form of GFP is 0.47 V (for the $GFP^{\bullet} + 1e \rightarrow GFP^{-}$ reaction), and the reduction potential at physiological conditions (pH 7, T = 25 °C) is 0.06 V.

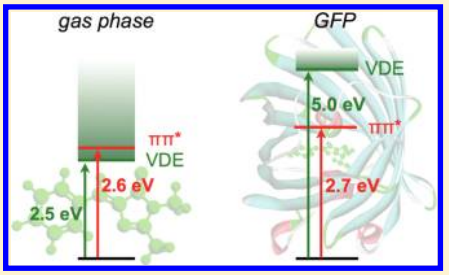

1. INTRODUCTION

The unique properties of green fluorescent protein (GFP) exploited in novel bioimaging techniques have revolutionized many areas in life sciences[1−3] and motivated numerous experimental and theoretical studies.[4−6] Yet, intrinsic electronic properties of the chromophores and their interactions with the protein matrix are not fully understood.

The gas-phase studies of model chromophores characterize intrinsic details of their electronic structure and provide important benchmarks for theory.[7−10] However, for a complete understanding of GFP photophysics, the characterization of chromophore−protein interactions is mandatory.

The protein environment plays a crucial role in the GFP photocycle. For example, the bare chromophore does not fluoresce in gas phase and solutions. The excited-state lifetime drops by 4 orders of magnitude, i.e., from nanoseconds in the protein to subpicosecond in solutions.[4] This dramatic change is attributed to the restricted range of motion of the chromophore in the protein, although the details of radiationless relaxation in protein and solutions have not yet been completely resolved.

The protein can also affect the energy and the character of excited states. Governed by electronic density distribution patterns, the protein-induced shifts may be nonuniform for different excited states thus changing the respective energy gaps and even the relative state ordering. Interestingly, gas-phase action spectroscopy experiments[7−9] on the GFP chromophore have reported a vertical excitation energy of 2.6 eV, which is remarkably close to the absorption maximum of GFP at 2.54 eV.[1] This finding has been confirmed by the QM/MM (quantum mechanics/molecular mechanics) calculations with the CASPT2 approach in the QM part,[11] which determined that the interactions with protein (in the so-called I-form referring to the resting anionic state of the chromophore) result in 0.02 eV red-shift relative to the isolated chromophore (this theoretical value agrees well with the experimental shift of 0.06 eV). Thus, the protein environment has a negligible effect on the excitation energy of the bright state.

One may expect a much stronger effect on the ionized states of the chromophore, and, consequently, electron detachment energies (DEs). A characteristic feature of the anionic forms of photoactive protein chromophores is their low DE.[12,13] For example, the vertical detachment energy (VDE) of deprotonated HBDI in gas phase is 2.5 eV,[9,12,14] which is below the vertical excitation energy of the bright state at 2.6 eV.[7−9] Thus, the bright state is a metastable state embedded in the photodetachment continuum. Such resonance states have finite lifetimes leading to spectral line broadening. Low DEs of the anionic chromophores may play a role[14] in the recently observed photoconversion (oxidative redding).[15] Thus, an important question is how the

Received: March 2, 2011
Revised: May 17, 2011
Published: May 18, 2011

protein environment affects the energy gap between the detached and electronically excited states.

In the context of the condensed-phase chemistry, reduction/oxidation potentials are used to characterize the propensity of molecules to accept or to donate electrons. VDE is related to the oxidation potential: smaller VDEs correspond to more positive values of the oxidation potential (or less positive/more negative values of the reduction potential for the inverse reaction). Thus, we also estimate the respective values of the GFP oxidation potential. The redox properties of the GFP chromophore have not yet been characterized quantitatively. Two studies have determined reduction potentials of the so-called redox-sensitive GFPs (roGFPs), which change the fluorsecense in response to the oxidation of the surface cysteine groups[16,17] (thus, the measured potentials correspond to the cysteine oxidation and not the chromophore). Another study reported reduction potential of the chromophore (resulting in the non-fluorescent form) in wtGFP.[18]

Singlet oxygen photosensitization by GFP and its mutants as well as formation of other reactive oxygen species (ROS) enables applications of GFPs in chromophore assisted laser inactivation.[19−22] Production of singlet oxygen reported for a number of GFP derivatives[19,21,23] points to a population of the excited triplet state of the chromophore. Moreover, triplets have been involved in a recently proposed mechanism of anaerobic photoswitching of GFP to a red-emitting form.[24] Thus, the characterization of the lowest triplet state is also of interest.

In addition to solvatochromic shifts of the chromophore's states, the protein may lead to new electronic states associated with the chromophore, which do not exist in the gas phase, such as CTTS (charge-transfer-to-solvent) states. The CTTS states, which are common in condensed phase, correspond to promoting an electron from an orbital localized on a chromophore to an orbital occupying nearby voids and stabilized by the interactions with solvent molecules.[25−28] They appear below the completely ionized states and are thought of as the gateway states for the production of solvated electrons.[29,30] For example, the DE of aqueous iodide[26] is considerably larger that the respective gas-phase value (7.2 eV versus 3.0 eV), and an optically bright CTTS band appears at 5.4 eV. The existence of a suitable nearby cavity (of 2−6 Å) is crucial for the CTTS state to exist.[26] In aqueous solutions, instantaneous voids appear due to the thermal fluctuations of solvent, however, in tightly packed proteins such cavities may not be available.

The focus of this work is on characterizing protein effects on the electronically excited and ionized states of the GFP chromophore and elucidation of the existence of CTTS states. We present the results of electronic structure calculations of the GFP chromophore in the protein environment using a variety of QM/MM approaches. While the excited states of the chromophores have been extensively characterized computationally[4,6] both in the gas-phase in and protein environment, the electron-detached states have began to attract attention only recently.[12,14] Experimentally, electron-detachment channel in the gas phase was characterized by Forbes and Jockusch.[9] Lukyanov and co-workers[15] discovered the ability of GFP to be a light-induced donor of electrons in their study of oxidative redding.[15] Based on the observation that this property is common to many diverse GFPs, they made an intriguing suggestion that this light-driven electron transfer may be a primary function of the GFP ancestor and that other secondary functions (i.e., participation in bioluminescence and protection from sunlight) evolved later.

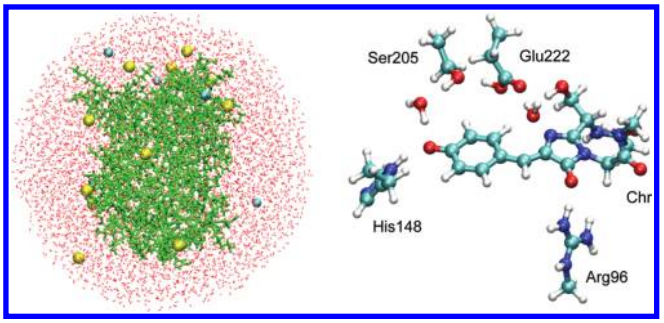

Figure 1. Left: Optimized structure of the GFP solvated in 6000 waters and 20 counterions. Right: The QM part mimicking the binding pocket of GFP. The chromophore is in the anionic form, the arginine residue is positively charged, and the rest of the residues in QM are neutral.

The production of solvated electrons (and transient absorption of the ionized deprotonated HBDI radical) have been observed for HBDI in solutions,[31,32] and it was suggested[31] that the ionization pathway may exist in GFP chromophore bound to the protein and that transient absorption at 1.97−2.48 eV observed in the pump−probe experiment[33] might be due to solvated electrons rather than excited-state absorption.[34] However, the CTTS states and production of solvated electrons in the GFP have not yet been observed experimentally.

2. COMPUTATIONAL DETAILS

The model system mimicking GFP was constructed based on the crystal structure 1EMA[35] from the PDB database.[36] This structure corresponds to the protein with a point mutation Ser65Thr from the wild-type GFP in which the chromophore is believed to be in the anionic form. The model exploited in the above-mentioned work of Olivucci et al.[11] relied on another PDB structure, 1GFL,[37] of the wild-type GFP, in which the chromophore is neutral and Glu222 is unprotonated. The coordinates of heavy atoms from the 1EMA structure were augmented by the hydrogen atoms, the side chain of the residue at the 65 position was set to Ser as in the wild type. We assumed that the Glu222 side chain was protonated, and the neutral form of His148 with the proton on the nitrogen atom oriented toward phenolate oxygen. Then the atomic coordinates of the model system were optimized by the QM/MM technique using the flexible effective fragment potential (EFP) method[38−40] with PBE0/6-31G(d) (ref 41) in the QM part and the *AMBER* force field parameters[42] in the MM part.

The chromophore and the side chains of Glu222, Arg96 and Ser205, His148 as well as two water molecules were assigned to the quantum subsystem, as shown in Figure 1. The chromophore is in the anionic form, and Arg96 is positively charged. Thus, the QM part is neutral. The atoms of the MM-part (2,181 in total) were grouped in 639 effective fragments (including 6 buffers) parameters of which were optimized previously.[43] The outer layer of the MM part was frozen, whereas the layer surrounding the QM part were allowed to relax in the geometry optimization. The details of the separation of the MM part into the frozen and flexible layers are given in the Supporting Information.

The QM/MM optimized model was augmented by the rest of the protein atoms from 1EMA PDB structure. The resulting system was extensively solvated by approximately 6000 water molecules, and the total charge on the protein was neutralized by

counterions: 13 positive and 7 negative counterions were added to neutralize locally negatively and positively charged surface residues. The solvation shell was first optimized (1000 optimization steps) and then equilibrated by molecular dynamics (MD) simulations. In the MD calculations, all protein atoms except the charged surface residues were frozen, and the solvent molecules and counterions were allowed to move. The constant temperature MD simulations were performed for the NVT ensemble at 300 K by using the Langevin thermostat. The simulations were carried out with a 1 fs integration step for 2 ns. All long-range electrostatic interactions were computed by using the particle mesh Ewald method. The constrains were imposed on the part of the protein taken from the equilibrium geometry configuration of the QM/MM model. The *NAMD 2.6* software suite[44] was used for MD simulations.

Twenty (each 100 ps) and 10 (each 200 ps) snapshots along the MD trajectory were used for VDE and excitation energy calculations, respectively. The average values computed along the MD trajectory are our best estimates (see the Supporting Information).

Figure 1 shows the entire solvated structure and the QM subsystem mimicking the chromophore binding pocket of the protein. These structures were used for vertical excitation and detachment energy calculations. To investigate the effect of different interactions on electronic states and the convergence of the results with respect to the system size, we also computed excitation and detachment energies in smaller clusters derived from the full QM system described above (e.g., chromophore + arginine, chromophore + arginine + water, etc.).

The excitation and detachment energies were computed using CIS, ωB97X-D,[45,46] and SOS-CIS(D).[47] We performed the following series of calculations: (i) bare model chromophore (deprotonated HBDI) at the geometry in the gas phase from ref 12 optimized by RI-MP2/cc-pVTZ; (ii) bare chromophore from the QM/MM model system (see Figure 1) at the geometry in the protein; (iii) series of QM calculations for the clusters of increasing size; (iv) QM/MM with the chromophore and selected neighboring residues in the QM part, and the rest of the protein/water/counterions described by point charges from the *CHARMM* force field.

Attachment/detachment density analysis[48] was used to characterize changes in electronic density upon electronic excitation in calculations (iii). In this approach the difference density matrix for the ground and excited states is decomposed into the detachment and attachment densities describing charge removal from the ground electronic state and its rearrangement in the excited electronic state.[48]

Calculations (i) and (ii) allowed us to quantify the shifts due to the chromophore geometry change in the protein (as well as the difference between HBDI and the chromophore representation in the QM/MM calculations). Calculations (iii) illuminated the effect of different residues on the relative positions of the detached and excited states.

As noted in ref 26, inclusion of long-range solvent electrostatic potential is essential for the converged detachment energies, e.g., the computed DE of iodine increased by about 2 eV when the first solvation shell of iodide and six water molecules (QM) was encapsulated in a cluster of additional 858 MM waters. Even slower convergence of VDE with respect to the model system size was reported in a recent computational study[49] in which the convergence of VDE of aqueous chloride required using the box size of 30 Å including about 4,000 water molecules. Relatively slow convergence of ionization energy with respect to the system size (a simulation box of 36 Å containing approximately 1,500 waters was used) was observed in a recent study of a neutral chromophore, a thymine molecule solvated in water.[50]

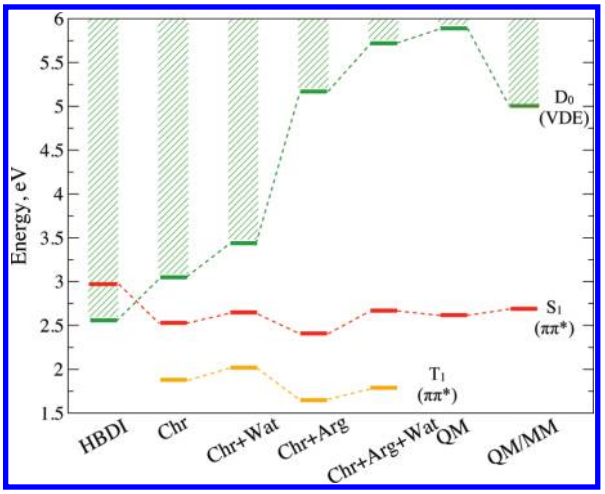

Figure 2. Energy diagram of the relevant electronic states of the bare HBDI chromophore and the chromophore in different environments.

We compute VDE and vertical excitation energies of the bright $\pi\pi^*$ state by using energy additivity approaches designed to take advantage of error cancellation, similarly to our calculations in refs 12, 14, 51, and 52. For example, neither DFT nor Hartree−Fock/Koopmans theorem (HF/KT) values of VDEs are sufficiently accurate, however, the effect of electron correlation can be estimated for the bare chromophore (HBDI) and then used to extrapolate the ωB97X/6-31+G(d,p) values computed for larger clusters. Likewise, the effect of increasing basis set can be estimated using HF/KT calculations.

To reliably estimate relative positions of different electronic states, we employ two complementary strategies. The first one is a brute-force approach: we compute vertical excitation energies of the valence and the CTTS-like excited states by using the SOS-CIS(D) method[47] with the 6-31(2+,+)G(d,p) basis set. The SOS-CIS(D) method has been found to yield accurate excitation energies for the valence states in several recent studies.[12,14,53,54] For the bright state of HBDI, the SOS-CIS(D)/aug-cc-pVTZ excitation energy is equal 2.72 eV, which is in excellent agreement with experimentally derived value and higher-level calculations.[12] However, we have to reduce the basis set size for calculations of larger clusters. We evaluate the effect of using reduced basis set by comparing the aug-cc-pVTZ and 6-31(2+,+)G(d,p) results for bare HBDI.

The results discussed below are our best estimates obtained using the above strategies. The raw data (ωB97X and HF/Koopmans VDEs, CIS excitation energies, etc.) are given in the Supporting Information. Calculations were performed with the *Q-CHEM*[55] and *PC-GAMESS*[56,57] electronic structure packages.

3. RESULTS AND DISCUSSION

Figure 2 shows energy levels of deprotonated HBDI in the gas phase[14] and in the protein environment as well as in the model QM clusters of increasing size. For the anionic form, the bright excited state is at 2.6 eV[12] vertically and the VDE is 2.5 eV. The excited state is derived by a $\pi\pi^*$-like excitation, and the detached

Table 1. Changes in VDE (eV) Relative to the Reference Value in the Gas-Phase Model Chromophore (Deprotonated HBDI) and the Extrapolated VDEs (eV)

system	ωB97X-D/6-31(+)G(d,p)	KT/6-31(+,+)G(d,p)	VDE (extrapolated)
HBDI	2.73	2.88	2.50[a]
Chr	+0.49	+0.67	2.99
Chr+Arg	+2.61	+2.98	5.11
Chr+Wat	+0.88	+1.06	3.38
Chr+His	+1.06	+1.27	3.56
Chr+Arg+Wat	+3.16	+3.34	5.66
Entire QM	+3.33	+3.56	5.83
QM/MM	+2.19 − +2.67		4.69−5.17
QM/MM, best estimate	+2.49		4.99

[a] The best estimate of HBDI VDE is 2.50 eV based on the following data: KT/6-31+G(d)=2.91 eV, EOM-IP/6-31+G(d)=2.48 eV, KT/6-311(2+,+)G(2df,2pd)=2.93 eV. The KT/6-31(2+,+)G(d,p) and KT/6-31(2+,2+)G(d,p) values are identical.

state corresponds to the removing an electron from the π orbital (π is the HOMO, and π^* is the valence LUMO).

In the protein, the energy of the $\pi\pi^*$ excited state is almost unchanged; however, the VDE increases up to 5.0 eV. The VDE is found to be quite sensitive to the positions of counterions and solvating water molecules, e.g., the VDEs computed for the several structures used in this study vary between 4.6−5.2 eV (5.0 is the best estimate, see section 2), whereas the $\pi\pi^*$ excitation energy varies between 2.68 and 2.74 eV.

To analyze the effect of different interactions, we first consider the dependence of VDE on the system size. Table 1 presents the changes in VDE relative to the reference HBDI computed using Koopmans theorem (KT) and as energy differences (ΔE scheme) using ωB97X-D. At the HF/KT level, the VDE does not change when the basis is increased from 6-31(+,+)G(d,p) to 6-31(2+,2+)G(d,p). The changes computed using ΔE scheme with ωB97X-D follow a similar trend, although they are 0.2 eV lower than the HF/KT values. Close inspection of Table 1 reveals that this difference is due to the discrepancy in the change of the VDE due to structural differences between gas-phase HBDI and the chromophore representation in the protein. Since the respective structures were computed using higher-level methods, we expect that ωB97X-D describes this change more reliably.

As one can see, adding positively charged arginine leads to the most significant change in VDE relative to the bare chromophore (about 3 eV). The cumulative effect of other neighboring residues in the QM part amounts to about 0.5 eV. However, the inclusion of the rest of the protein is important for the converged result leading to the −0.8 eV change in VDE relative to the QM part. As mentioned above, the VDE is very sensitive to the positions of solvating water molecules and counterions outside the β barrel despite a large size of the system ($R \sim 36$ Å). The magnitude of the observed variations (up to 0.5 eV) suggests that thermal fluctuations will strongly modulate the VDE. The inclusion of the entire protein and water/counterions in QM/MM results in the VDE decrease relative to the QM value. This is because the stabilizing effect of the nearby charged arginine becomes partially screened by the environment.

The converged VDE value in QM/MM (using averaged value along MD trajectory, see section 2) is 5.22 eV at the ωB97X-D/6-31(+)G(d,p) level. To account for electron correlation/basis set, we correct this value by the difference of the respective VDEs of HBDI with our reference value of 2.50 eV from refs.[12,14] which includes EOM-IP (equation-of-motion coupled-cluster method for ionization potentials, see, for example, ref 58) correction and basis set extrapolation. Our best estimates for absolute values of VDEs of model clusters are obtained by adding −0.23 eV correction, the difference between the extrapolated VDE of HBDI and the respective ωB97X/6-31(+)G(d,p) value, to the respective ωB97X/6-31(+)G(d) VDEs. The HF/KT values can be similarly adjusted by using −0.38 eV correction giving rise to the VDEs which are 0.2 eV higher that those computed with ωB97X/6-31(+)G(d,p).

Thus, we arrive to 4.99 eV as our best estimate of the VDE of the anionic GFP chromophore in the solvated protein environment.

Table 2. Vertical Excitation Energies of the Bright $^1\pi\pi^*$ State and $^3\pi\pi^*$ Computed by SOS-CIS(D) with the 6-31(2+,+)G(d,p) Basis Set[a]

system	$^1\pi\pi^*$	$^3\pi\pi^*$
HBDI	2.62 (1.54)[b]	1.86[b]
Chr	2.47 (1.34)	1.82
Chr+Arg	2.35 (1.61)	1.59
Chr+Wat	2.59 (1.24)	1.96
Chr+Arg+Wat[b]	2.61 (0.95)	1.73
Chr+Arg+His+Wat	2.41 (1.64)	
QM	2.56 (1.48)	
QM/MM	2.68−2.74	
QM/MM, best estimate	2.70	

[a] Oscillator strengths (CIS) are given in parentheses. [b] SOS-CIS(D)/cc-pVTZ, ref 12.

The excitation energy of the bright state is less sensitive to the environment, in agreement with ref 11, and in spite of different starting models. Table 1 shows that 0.1−0.2 eV changes due to the interactions with nearby residues and structural changes of the chromophore cancel out resulting in essentially the same value as in the gas phase. The converged value of excitation energy in the protein 2.70 eV is in good agreement with experimental data 2.51 and 2.54 eV for wild-type GFP (B band) and EGFP, respectively.[1,2]

The effect of the protein environment on the lowest triplet state of the chromophore (see Table 2 and Figure 2) is very similar to that of the singlet state, which is not surprising given that the two states are derived from the same pair of orbitals. The computed energy of T_1 in the largest considered model

(Chr+Arg+Wat) is 1.73 eV, which is slightly below the value reported[12] for HBDI, 1.84 eV [SOS-CIS(D)/cc-pVTZ, ref 12].

3.1. Do CTTS States Exist in the Protein? As evident from the energy diagram shown in Figure 2, the energy gap (>2 eV) between the bright excited state of the chromophore and detachment continuum suggests possible existence of the CTTS states, which commonly occur in polar solutions.[25−28] We investigated the intriguing possibility of finding such states in the protein by performing excited state calculations on the clusters of increasing size using the bases sets augmented by several diffuse sets.[12] The CTTS states would appear as excited states with low (but nonzero) oscillator strength at energies below VDE, and their wave functions should feature a diffuse target orbital in a proximity of the chromophore. The excitation energy of these CTTS states can be computed directly by, for example, SOS-CIS(D) method, or in a two-step procedure combining the CIS estimate of the so-called vertical binding energy (VBE) of the CTTS state (the difference between the CIS energy of this state and the Koopmans VDE) with an accurate value of VDE. Whereas the absolute CIS excitation energies are rather crude, the CIS VBEs are found to be accurate. For example, in our model systems the excitation energies of the CTTS states computed with SOS-CIS(D) are within 0.2 eV from the values estimated based on the CIS VBEs. The results for a series of such calculations for molecular clusters including the chromophore are given in Supporting Information; here we only summarize the main conclusions.

In small clusters (Chr+Wat, Chr+Arg, Chr+Arg+Wat), CTTS states appear at 2.7−3.1 eV (the respective VBE varies from 0.1 to 2.5 eV), as shown in Figure 3 and Table 3. The wave function analysis using attachment-detachment densities reveals that the target orbital resides near the positively charged arginine residue. Note that in the Chr-Arg-Wat cluster, the $\pi\pi^*$ and the CTTS states happen to be degenerate at the CIS level, and their wave functions are strongly mixed. The degeneracy is removed at the SOS-CIS(D) level, however, owing to a perturbative character of (D), the SOS-CIS(D) results should be considered with caution in this case.

As quantum system is increased, the CTTS states are pushed outside the QM region, and no CTTS excited states at energies below the respective VDEs are found with electron density localized inside the QM part. Note that typical size of the cavities required to accommodate solvated electrons is about 4 Å in diameter.[30,59−62] A basic cavity analysis of the GFP crystallographic structure (PDB ID 1EMA) performed using the *SPDBV 4.01* software has shown that the cavities in the proximity of the chromophore (within 10 Å) are less than 4 Å in diameter and are, therefore, too small to accommodate a CTTS electron. Thus, we conclude that a tightly folded structure of this GFP does not have cavities that could support CTTS states. However, other mutants may have water-filled cavities that are sufficiently large to accommodate CTTS states.

3.2. Effect of Hydrogen Bonding on the Electron-Detached and Valence Excited States. As demonstrated above, the interactions with protein matrix and a nearby water molecule strongly affect the relative ordering of the ionized and excited states. In this section, we focus on the interactions of the chromophore with one water molecule. As revealed by the crystal structure, there is a water molecule hydrogen-bonded to the phenolate oxygen. In the QM/MM optimized structure (see Figure 1), the distance between the water's oxygen and phenolate oxygen atoms is 2.60 Å. Not surprisingly, the lowest energy

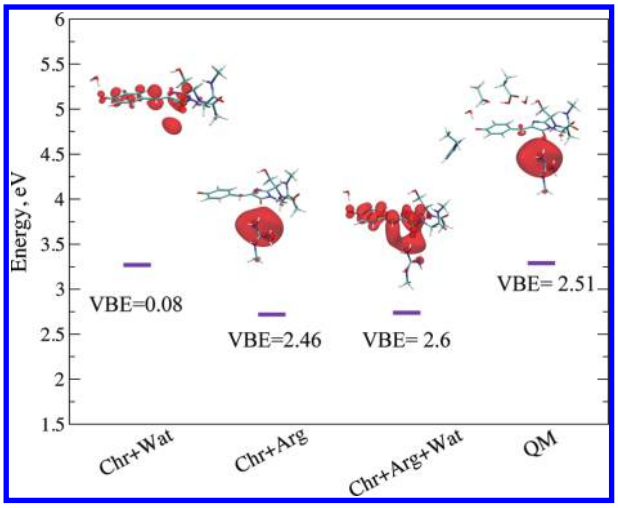

Figure 3. Excitation energies of a CTTS-like state [SOS-CIS(D)/6-31(2+,+)G(d,p)] in different QM clusters mimicking the GFP active site. The CIS binding energies (eV) of the CTTS states and the attachment densities of the CIS wave function are also shown.

Table 3. VBE (eV) of the Lowest CTTS-Like State Computed by CIS[a]

system	6-31(+,+)G(d,p)	6-31(2+,+)G(d,p)	6-31(2+,2+)G(d,p)
Chr+Arg	2.36 (0.05)	2.46 (0.01)	2.46 (0.01)
Chr+Wat[b]	−0.30	0.08	0.11
Chr+His	−0.15 (0.01)	0.20 (0.05)	0.19 (0.05)
Chr+Arg+Wat[b]		2.55−2.59	

[a] The oscillator strengths of the CTTS state is given in parentheses. [b] The CTTS state is strongly mixed with the bright state leading to intensity borrowing.

isomer of monohydrated HBDI also features water at the phenolate end (the respective H···O distance is 1.732 Å).[63] The effect of microhydration on the excitation energy is rather small, i.e., in the gas-phase structure, it results in 0.04 eV blue shift [computed by SOS-CIS(D)/6-31+G(d,p)]. However, VDE is blue-shifted by 0.36 eV due to stabilizing effect of microhydration on the anionic species. Thus, a single water molecule is sufficient to convert the $\pi\pi^*$ state from a resonance into a bound state.

We observe similar effect of hydrogen bonding for the chromophore-water model structure from the QM/MM calculations (see Table 1). The VDE of Chr-Wat cluster is 0.39 eV higher than that of the bare chromophore. Interestingly, the h-bonding has even stronger effect on the VDE of the Chr-Arg cluster (characterized by relatively large VDE of 5.11 eV); adding water to this system increases the VDE by 0.55 eV.

By changing the gap between the detached and the $\pi\pi^*$ state, the interactions with water molecule also affect the CTTS-like state. An interesting effect is observed in Chr-Arg-Wat model system, where the $\pi\pi^*$ and the CTTS-like states are happen to be degenerate at the CIS level, and their wave functions become strongly mixed (see Figure 3 and Table 3). Consequently, the oscillator strengths is split almost equally between these two states (0.67 and 0.92). This accidental degeneracy can be removed by varying the Chr-Wat distance (see the Supporting Information).

To analyze the effect of hydrogen bonding on the CTTS-like state, we performed a series of calculations for the Chr+Arg+Wat and Chr-Wat model systems with O(Chr)−O(Wat) distance gradually increased from 2.6 to 3.65 Å (see Supporting Information). As H_2O is pulled away from the chromophore, the VDE decreases approaching the respective Chr (or Chr-Arg) values. The CTTS-like state closely follows the VDE trend, thus, its VBE remains nearly constant (2.50−2.59 eV in Chr+Arg+Wat) in this range of hydrogen bond length. The energy of the $\pi\pi^*$ state slightly decreases.

3.3. Standard Oxidation Potential of the Anionic Form of GFP. Standard oxidation potential of anionic GFP

$$GFP^- \rightarrow GFP^\bullet + e^- \quad (1)$$

is of interest in connection to the so-called oxidative redding,[14,15] a new type of photoconversion. Lukyanov and co-workers have discovered that in the presence of oxidants and upon illumination by 488 nm (2.54 eV) light, EGFP and a number of other GFP mutants are converted to a red-emitting form.[15] GFP irradiated by 488 nm (2.54 eV) light was reported to reduce a number of biologically relevant electron acceptors including cytochrome *c* ($E^{\circ\prime}$ = 0.22 V), flavin mononucleotide (FMN, $E^{\circ\prime}$ = −0.22 V), and nicotinamide dinucleotide (NAD^+, $E^{\circ\prime}$ = −0.32).[15] The standard reduction potentials are from Supporting Materials of ref 15. The first step in elucidating the mechanism of oxidative redding is, therefore, to test whether GFP can be oxidized in its ground electronic state or the above oxidative agents can only remove an electron from the electronically excited chromophore. Moreover, the redox properties of GFP may be of a broader significance, e.g., in a context of its potential role as a light-driven electron donor[15] or fluorescent redox sensors.[16,17]

Calculations of standard reduction potentials (E°) require estimation of the free energy difference for reaction (1), and differential free energy for the solvation of GFP^- and the respective oxidized species, GFP.

Neglecting ΔpV and entropic terms (i.e., assuming that $\Delta H_r^0 = \Delta E_r$ and $\Delta S_r^0 = 0$), the free energy change of reaction (1) can be approximated by adiabatic detachment energy (ADE). We computed ADE by using the best estimate of the VDE given in Table 1 and the relaxation energy (i.e., ground-state energy difference of $GFP^\bullet$ at the optimized geometries of the original anionic structure and the electron-detached radical). The geometry of electron-detached GFP was optimized using the same QM/MM model as for anionic GFP. Then single point ωB97X-D/6-31+G(d,p) calculations were performed for $GFP^\bullet$ at both equilibrium geometries using cluster model with the quantum part geometry extracted from the QM/MM optimized structures. The resulting relaxation energy is 0.16 eV, which is very close to the gas-phase value 0.15 eV reported in ref 14. The ADE derived using our best estimate of VDE (4.99 eV) is thus 4.83 eV.

E°, the reduction potential with respect to the standard hydrogen electrode, is defined as follows:

$$E^\circ = -\frac{\Delta G^\circ}{nF} \quad (2)$$

where ΔG° is the difference of the negative of the free energy change for half-reaction (1) approximated by negative of ADE and proton one-electron reduction (−4.36 eV, ref 64). This yields E° = 0.47 V.

For the biological applications,[16,17] it is more appropriate to consider reduction potential at the physiological conditions, $E^{\circ\prime}$, that is at pH = 7 and T = 25 °C. This potential can be computed from $E^\circ \equiv E(\text{pH } 0)$ by using the Nernst equation:

$$E^{\circ\prime} = E^\circ - 0.059 \times \text{pH} \quad (3)$$

where $E^{\circ\prime}$ and E° are measured in V. Using eq 3 we neglect the effects of the pH change on the protonation state of the protein acidic/basic residues, which can influence ionization energy of the chromophore. Since in our calculations, we employed the protein model in the standard protonation states, it is appropriate to report $E^{\circ\prime}$ computed using eq 3, with the understanding that our E° is an extrapolation to the pH 0. The computed $E^{\circ\prime}$ is 0.06 V.

The E° value can be compared with a cruder estimate obtained using an empirical calibration scheme[65] based on computed VDEs

$$E^{\circ,ox} = (-2.59 \pm 0.26) + (0.56 \pm 0.03) \times \text{VIE} \quad (4)$$

which results in $E^\circ = -0.20 \pm 0.41$ V.

As discussed above, the computed VDEs are sensitive to the representation of the environment (solvent, counterions), and, therefore, E° can vary within the range of the VDEs given in Table 1. For the lowest and highest QM/MM VDEs (Table 1), E° calculated using eq 2 are 0.17 and 0.65 V, respectively. These variations provide a conservative estimate of the error bar for the computed E°.

Thus, the computed E° values show that GFP in the ground electronic states is not able to reduce the compounds with E° below 0.17 V ($E^{\circ\prime}$= −0.24). Therefore, electronic excitation is required to initiate oxidative redding.

The computed $E^{\circ\prime}$ value of 0.06 V is more positive than $E^{\circ\prime}$ of roGFP (−0.3 V) corresponding to the two-electron surface cysteine group oxidation.[16,17] Thus, the calculations predict that the anionic chromophore is a weaker reducing agent than the surface cysteine groups, which is consistent with the fact that chromophore is not oxidized in roGFPs.

It is also instructive to compare the computed E° with similar systems. For example, deprotonated phenol ($PheO^-$) can be considered as a model system representing the anionic GFP chromophore. The gas-phase adiabatic DEs for the phenolate and deprotonated HBDI are close: 2.253[66] and 2.39 eV,[14] however, the computed standard reduction potential of GFP (E° = 0.47 V) is much lower than the high pH E° values of phenol in aqueous solutions (the reported experimental standard reduction potential for the $PheO^\bullet/PheO^-$ pair vary in the range 0.79−0.86 V[67−69]). This is because the differential solvation contribution to the standard reduction potential differ significantly for bare $PheO^-$ in polar water solution and negatively charged GFP chromophore shielded by the protein matrix. One can expect that deprotonated HBDI in water would have E° much closer to that of phenolate. The stronger solvent stabilization of the anion in water (relative to the protein environment) would make aqueous deprotonated HBDI a weaker reducing agent than GFP. However, chromophore's shielding by the protein may strongly affect the kinetics of the electron transfer thus reducing the efficiency of the oxidation process.

In sum, the protein environment may play a dual role in the redox properties of GFP. Thermodynamically, interactions with the protein increase the reducing ability of GFP (relative to the bare chromophore in water), however, kinetically, the protein shielding protects the chromophore from oxidation. The kinetic

dx.doi.org/10.1021/jp2020269 |J. Phys. Chem. B 2011, 115, 8296–8303

effect may be responsible for the absence of solvated electrons in GFP experiments,[34] in contrast to the solvated HBDI studies.[31,32]

As far as oxidative redding is concerned, more detailed analysis including estimation of standard oxidation potential of electronically excited GFP is required for its mechanistic understanding.

4. CONCLUSIONS

We investigated the effect of the protein environment on the electronic properties of the GFP chromophore. While the protein has a very small effect on the character and excitation energy of the singlet and triplet $\pi\pi^*$ states of GFP, its effect on the VDE is more significant (the VDE increases from 2.5 eV in the gas phase to 5.0 eV in the solvated protein). Based on the analogy with aqueous anions, we expect that VDE of the bare chromophore is aqueous solution would be even larger owing to more efficient stabilization of the anionic species in polar solvents.

To analyze redox properties of GFP, we estimated standard reduction potential of GFP in its ground state, which is found to be E° = 0.47 V (the respective value at the physiological conditions is $E^{\circ\prime}$ = 0.06 V). This E° value is smaller than that of the aqueous phenolate (which is similar to deprotonated HBDI and has especially the same gas-phase VDE). Thus, the interactions with the protein increase the reducing ability of GFP (relative to the bare chromophore in water), although kinetically, the protein may slow down the oxidation reaction by shielding the chromophore.

We also investigated the possible existence of the CTTS states and found that a tightly packed GFP does not present cavities suitable to accommodate a CTTS electron. However, GFP mutants with larger water-filled cavities in the vicinity of the chromophore (such as KillerRed) may be able to support the CTTS states.

■ ASSOCIATED CONTENT

Supporting Information. Compilation of raw data used in estimates of VDE and excitation energies; attachment−detachment density analysis of the electronic states in cluster models and results of the calculations in the model systems with varying water−chromophore distance; relevant Cartesian geometries. This material is available free of charge via the Internet at http://pubs.acs.org.

■ ACKNOWLEDGMENT

This work was conducted under the auspices of the *iOpenShell* Center for Computational Studies of Electronic Structure and Spectroscopy of Open-Shell and Electronically Excited Species (http://iopenshell.usc.edu) supported by the National Science Foundation through the CRIF:CRF CHE-0625419 + 0624602 + 0625237 grant, as well as through the CHE-0951634 (AIK) grant. This work is also supported by the Russian Foundation for Basic Research (project 10-03-0085). M.K. acknowledges partial support from the grant MK-64815.2010.4 We thank Profs. Steven E. Bradforth (USC) and Delmar Larsen (UC Davis) for stimulating discussions.

■ REFERENCES

(1) Tsien, R. Y. *Annu. Rev. Biochem.* **1998**, *67*, 509.
(2) Zimmer, M. *Chem. Rev.* **2002**, *102*, 759.
(3) Wang, Y.; Shyy, J.Y.-J.; Chien, S. *Ann. Rev. Biomed. Eng.* **2008**, *10*, 1.
(4) Meech, S. R. *Chem. Soc. Rev.* **2009**, *38*, 2922.
(5) Sample, V.; Newman, R. H.; Zhang, J. *Chem. Soc. Rev.* **2009**, *38*, 2852.
(6) Nemukhin, A. V.; Grigorenko, B. L.; Savitskii, A. P. *Acta Naturae* **2009**, *2*, 41.
(7) Nielsen, S. B.; Lapierre, A.; Andersen, J. U.; Pedersen, U. V.; Tomita, S.; Andersen, L. H. *Phys. Rev. Lett.* **2001**, *87*, 228102.
(8) Andersen, L. H.; Lappierre, A.; Nielsen, S. B.; Nielsen, I. B.; Pedersen, S. U.; Pedersen, U. V.; Tomita, S. *Eur. Phys. J. D* **2002**, *20*, 597.
(9) Forbes, M. W.; Jockusch, R. A. *J. Am. Chem. Soc.* **2009**, *131*, 17038.
(10) Rajput, J.; Rahbek, B., D.; Rocha-Rinza, L. H.; Andin, A. V.; Bochenkova, A. V.; Solntsev, K. M.; Dong, J.; Kowalik, J.; Tolbert, L. M.; Åxman Petersen, M.; Brøndsted Nielsen, M. *Phys. Chem. Chem. Phys.* **2009**, *11*, 9996.
(11) Sinicropi, A.; Anduniow, T.; Ferre, N.; Basosi, R.; Olivucci, M. *J. Am. Chem. Soc.* **2005**, *127*, 11534.
(12) Epifanovsky, E.; Polyakov, I.; Grigorenko, B. L.; Nemukhin, A. V.; Krylov, A. I. *J. Chem. Theory Comput.* **2009**, *5*, 1895.
(13) Zuev, D.; Bravaya, K. B.; Crawford, T. D.; Lindh, R.; Krylov, A. I. *J. Chem. Phys.* **2011**, *134*, 034310.
(14) Epifanovsky, E.; Polyakov, I.; Grigorenko, B. L.; Nemukhin, A. V.; Krylov, A. I. *J. Chem. Phys.* **2010**, *132*, 115104.
(15) Bogdanov, A. M.; Mishin, A. S.; Yampolsky, I. V.; Belousov, V. V.; Chudakov, D. M.; Subach, F. V.; Verkhusha, V. V.; Lukyanov, S.; Lukyanov, K. A. *Nat. Chem. Biol.* **2009**, *5*, 459.
(16) Hanson, G. T.; Aggeler, R.; Oglesbee, D.; Cannon, M.; Capaldi, R. A.; Tsien, R. Y.; Remington, S. J. *J. Biol. Chem.* **2004**, *279*, 13044.
(17) Dooley, C. T.; Dore, T. M.; Hanson, G. T.; Jakson, W. C.; Remington, S. G.; Tsien, R. Y. *J. Biol. Chem.* **2004**, *279*, 2284.
(18) Inouye, S.; Tsuji, F. I. *FEBS Lett.* **1994**, *351*, 211.
(19) Jiménez-Banzo, A.; Ragás, X.; Abbruzzetti, S.; Viappiani, C.; Campanini, B.; Flors, C.; Nonell, S. *Photochem. Photobiol. Sci.* **2010**, *9*, 1336.
(20) Vegh, R. B.; Solntsev, K. M.; Kuimova, M. K.; Cho, S.; Liang, Y.; Loo, B. L. W.; Tolbert, L. M.; Bommarius, A. S. *Chem. Commun.* **2011**, *47*, 4887.
(21) Ragás, X.; Cooper, L. P.; White, J. H.; Nonell, S.; Flors, C. *ChemPhysChem* **2011**, *12*, 161.
(22) McLean, M. A.; Rajfur, Z.; Chen, Z.; Humphrey, D.; Yang, B.; Sligar, S. G.; Jacobson, K. *Anal. Chem.* **2009**, *81*, 1755.
(23) Bell, A. F.; Stoner-Ma, D.; Wachter, R. M.; Tonge, P. J. *J. Am. Chem. Soc.* **2003**, *125*, 6919.
(24) Koseki, J.; Kita, Y.; Tachikawa, M. *Biophys. Chem.* **2010**, *147*, 140.
(25) Blandamer, M. J.; Fox, M. F. *Chem. Rev.* **1970**, *70*, 59.
(26) Bradforth, S. E.; Jungwirth, P. *J. Phys. Chem. A* **2002**, *106*, 1286.
(27) Simons, J. *J. Phys. Chem. A* **2008**, *112*, 6401.
(28) Sobolewski, A. L.; Domcke, W. *Phys. Chem. Chem. Phys.* **2007**, *9*, 3818.
(29) Feng, D. F.; Kevan, L. *Chem. Rev.* **1980**, *80*, 1.
(30) Jacobson, L. D.; Herbert, J. M. *J. Am. Chem. Soc.* **2010**, *132*, 10000.
(31) Vengris, M.; van Stokkum, I. H. M.; He, X.; Bell, A. F.; Tonge, P.; van Grondelle, R.; Larsen, D. S. *J. Phys. Chem. A* **2004**, *108*, 4587.
(32) Solntsev, K. M.; Poizat, O.; Dong, J.; Rehault, J.; Lou, Y.; Burda, C.; Tolbert, L. M. *J. Phys. Chem. B* **2008**, *112*, 2700.
(33) Winkler, K.; Lindner, J.; Subramaniam, V.; Jovin, T. M. *Phys. Chem. Chem. Phys.* **2002**, *4*, 1072.
(34) No two-photon ionization was observed in subsequent experiments using 400 nm laser (total energy of 6.2 eV) (D. Larsen, private communication).
(35) Ormö, M.; Cubitt, A. B.; Kallio, K.; Gross, L. A.; Tsien, R. Y.; Remington, S. J. *Science* **1996**, *273*, 1392.
(36) http://www.rcsb.org/.
(37) Yang, F.; Moss, L. G.; Phillips, G. N. *Nat. Biotechnol.* **1996**, *14*, 1246.
(38) Gordon, M. S.; Freitag, M. A.; Bandyopadhyay, P.; Jensen, J. H.; Kairys, V.; Stevens, W. J. *J. Phys. Chem. A* **2001**, *105*, 293.

(39) Adamovic, I.; Freitag, M. A.; Gordon, M. S. *J. Chem. Phys.* **2003**, *118*, 6725.
(40) Nemukhin, A. V.; Grigorenko, B. L.; Topol, I. A.; Burt, S. K. *J. Comput. Chem.* **2003**, *24*, 1410.
(41) Adamo, C.; Barone, V. *J. Chem. Phys.* **1999**, *110*, 6158.
(42) Case, D. A. ; Darden, T. A. ; III, Cheetham, T.E.; ; Simmerling, C. L. ; Wang, J. ; Duke, R. E. ; Luo, R. ; Merz, K. M. ; Wang, B. ; Pearlman, D. A. ; Crowley, M. ; Brozell, S. ; Tsui, V. ; Gohlke, H. ; Mongan, J. ; Hornak, V. ; Cui, G. ; Beroza, P. ; Schafmeister, C. ; Caldwell, J. W. ; Ross, W. S. ; Kollman, P. A. *Amber 8*; University of California: San Francisco, 2004.
(43) Grigorenko, B.; Savitsky, A.; Topol, I.; Burt, S.; Nemukhin, A. *J. Phys. Chem. B* **2006**, *110*, 18635.
(44) Phillips, J. C.; Braun, R.; Wang, W.; Gumbart, J.; Tajkhorshid, E.; Villa, E.; Chipot, C.; Skeel, R. D.; Kale, L.; Schulten, K. *J. Comput. Chem.* **2005**, *26*, 1781.
(45) Chai, J.-D.; Head-Gordon, M. *J. Chem. Phys.* **2008**, *128*, 084106.
(46) Extensive benchmark study[45] of long-range corrected functionals has demonstrated improved accuracy for a variety of thermochemical properties including ionization energies relative to their nonlong-range corrected counterparts (e.g., wB3LYP versus B3LYP). Among the functionals tested, wB97X has been shown to yield the best results. Thus, we employ this functional in our study.
(47) Rhee, Y. M.; Head-Gordon, M. *J. Phys. Chem. A* **2007**, *111*, 5314.
(48) Head-Gordon, M.; Grana, A. M.; Maurice, D.; White, C. A. *J. Phys. Chem.* **1995**, 14261.
(49) Cauët, E.; Valiev, M.; Weare, J. H. *J. Phys. Chem. B* **2010**, *114*, 5886.
(50) Ghosh, D. ; Isayev, O. ; Slipchenko, L. V. ; Krylov, A. I. *J. Phys. Chem. A* **2011**, 10.1021/jp110438c.
(51) Golubeva, A. A.; Krylov, A. I. *Phys. Chem. Chem. Phys.* **2009**, *11*, 1303.
(52) Bravaya, K. B.; Kostko, O.; Ahmed, M.; Krylov, A. I. *Phys. Chem. Chem. Phys.* **2010**, *12*, 2292.
(53) Polyakov, I.; Grigorenko, B. L.; Epifanovsky, E.; Grigorenko, B. L.; Krylov, A. I.; Nemukhin, A. V. *J. Chem. Theory Comput.* **2010**, *6*, 2377.
(54) Khrenova, M.; Nemukhin, A. V.; Grigorenko, B. L.; Krylov, A. I.; Domratcheva, T. *J. Chem. Theory Comput.* **2010**, *6*, 2293.
(55) Shao, Y.; Molnar, L. F.; Jung, Y.; Kussmann, J.; Ochsenfeld, C.; Brown, S.; Gilbert, A. T. B.; Slipchenko, L. V.; Levchenko, S. V.; O'Neil, D. P.; Distasio, R. A., Jr.; Lochan, R. C.; Wang, T.; Beran, G. J. O.; Besley, N. A.; Herbert, J. M.; Lin, C. Y.; Van Voorhis, T.; Chien, S. H.; Sodt, A.; Steele, R. P.; Rassolov, V. A.; Maslen, P.; Korambath, P. P.; Adamson, R. D.; Austin, B.; Baker, J.; Bird, E. F. C.; Daschel, H.; Doerksen, R. J.; Drew, A.; Dunietz, B. D.; Dutoi, A. D.; Furlani, T. R.; Gwaltney, S. R.; Heyden, A.; Hirata, S.; Hsu, C.-P.; Kedziora, G. S.; Khalliulin, R. Z.; Klunziger, P.; Lee, A. M.; Liang, W. Z.; Lotan, I.; Nair, N.; Peters, B.; Proynov, E. I.; Pieniazek, P. A.; Rhee, Y. M.; Ritchie, J.; Rosta, E.; Sherrill, C. D.; Simmonett, A. C.; Subotnik, J. E.; Woodcock, H. L., III; Zhang, W.; Bell, A. T.; Chakraborty, A. K.; Chipman, D. M.; Keil, F. J.; Warshel, A.; Herhe, W. J.; Schaefer, H. F., III; Kong, J.; Krylov, A. I.; Gill, P. M. W.; Head-Gordon, M. *Phys. Chem. Chem. Phys.* **2006**, *8*, 3172.
(56) Schmidt, M. W.; Baldridge, K. K.; Boatz, J. A.; Elbert, S. T.; Gordon, M. S.; Jensen, J. H.; Koseki, S.; Mastunaga, N.; Nguyen, K. A.; Su, S.; Windus, T. L.; Dupuis, M.; Montgomery, J. A. *J. Comput. Chem.* **1993**, *14*, 1347.
(57) Granovsky, A.A. PC GAMESS/Firefly, U. R. L. http://classic.chem.msu.su/gran/gamess/index.html (Accessed Dec. 18, 2009).
(58) Krylov, A. I. *Annu. Rev. Phys. Chem.* **2008**, *59*, 433.
(59) Kevan, L. *Acc. Chem. Res.* **1981**, *14*, 138.
(60) Bartels, D. M.; Takahashi, K.; Cline, J. A.; Marin, T. W.; Jonah, C. D. *J. Phys. Chem. A* **2005**, *109*, 1299.
(61) Jordan, K. D.; Johnson, M. A. *Science* **2010**, *329*, 42.
(62) Herbert, J. M.; Jacobson, L. D. *Int. Rev. Phys. Chem.* **2011**, *30*, 1.
(63) Zuev, D.; Bravaya, K.; Makarova, M.; Krylov, A. I. 2011; in preparation.
(64) Lewis, A.; Bumpus, J. A.; Thrular, D. G.; Cramer, C. J. *J. Chem. Educ.* **2004**, *81*, 596.
(65) Crespo-Hernández, C.; Close, D. M.; Gorb, L.; Leszczynski, J. *J. Phys. Chem. B* **2007**, *111*, 5386.
(66) Gunion, R. F.; Gilles, M. K.; Polak, M. L.; Lineberger, W. C. *Int. J. Mass Spectrom. Ion Proc.* **1992**, *117*, 601.
(67) Lind, J.; Shen, X.; Eriksen, T. E.; Merényi, G. *J. Am. Chem. Soc.* **1990**, *112*, 479.
(68) Li, C.; Hoffman, M. Z. *J. Phys. Chem. B* **1999**, *103*, 6653.
(69) Costentin, C.; Louault, C.; Savéant, J.-M. *Proc. Natl. Acad. Sci.* **2009**, *106*, 18143.